Calcif Tissue Int (2005) 76:207–213
DOI: 10.1007/s00223-004-0168-z

Calcified Tissue International

Bone Chemical Structure Response to Mechanical Stress Studied by High Pressure Raman Spectroscopy

O. de Carmejane,[1] M. D. Morris,[1] M. K. Davis,[2] L. Stixrude,[2] M. Tecklenburg,[3] R. M. Rajachar,[4,5] D. H. Kohn[4,5]

[1]Department of Chemistry, University of Michigan, Ann Arbor, MI, USA
[2]Department of Geological Sciences, University of Michigan, Ann Arbor, MI, USA
[3]Department of Chemistry, Central Michigan University, Ann Arbor, MI, USA
[4]Departments of Biologic and Material Sciences, University of Michigan, Ann Arbor, MI, USA
[5]Biomedical Engineering, University of Michigan, Ann Arbor, MI, USA

Received: 15 August 2004 / Accepted: 7 October 2004 / Online publication: 8 March 2005

Abstract. While the biomechanical properties of bone are reasonably well understood at many levels of structural hierarchy, surprisingly little is known about the response of bone to loading at the ultrastructural and crystal lattice levels. In this study, our aim was to examine the response (i.e., rate of change of the vibrational frequency of mineral and matrix bands as a function of applied pressure) of murine cortical bone subjected to hydrostatic compression. We determined the relative response during loading and unloading of mineral vs. matrix, and within the mineral, phosphate vs. carbonate, as well as proteinated vs. deproteinated bone. For all mineral species, shifts to higher wave numbers were observed as pressure increased. However, the change in vibrational frequency with pressure for the more rigid carbonate was less than for phosphate, and caused primarily by movement of ions within the unit cell. Deformation of phosphate on the other hand, results from both ionic movement as well as distortion. Changes in vibrational frequencies of organic species with pressure are greater than for mineral species, and are consistent with changes in protein secondary structures such as alterations in interfibril cross-links and helix pitch. Changes in vibrational frequency with pressure are similar between loading and unloading, implying reversibility, as a result of the inability to permanently move water out of the lattice. The use of high pressure Raman microspectroscopy enables a deeper understanding of the response of tissue to mechanical stress and demonstrates that individual mineral and matrix constituents respond differently to pressure.

Key words: Raman spectroscopy — Bone — Biomechanics — Diamond anvil cell — High pressure

The chemical composition and crystal structure of bone play an essential role in its biological and structural functions [1, 2]. Bone tissue can be described as a composite of an organic matrix reinforced with an inorganic mineral phase. The organic matrix is about 90% type I collagen fibrils locally oriented predominantly parallel to each other (in long bone) that provide a supporting matrix upon which the mineral crystals grow. The mineral fraction of bone is a highly impure carbonated apatite situated between collagen fibril cross-links and fibril ends. Both the organic and mineral components and the interactions between the two contribute to bone's mechanical properties, including strength, toughness and elasticity. It is not clear though how mineral crystallites deform in response to mechanical loading nor how the matrix deforms. This is particularly true at the atomic level. To better understand deformation it is useful to extract atomic-level compositional information about the changes in inorganic and organic phases that occur when bone undergoes mechanical loading.

Raman spectroscopy is a powerful technique for relating bone mechanical properties with bone ultrastructural and crystal lattice changes [3]. Raman spectroscopy provides bone vibrational spectra and, like infrared spectroscopy, it is nondestructive and provides simultaneous information about bone mineral and organic matrix. Raman spectroscopy has the advantages that it is equally applicable to thin and thick specimens, suffers no interference from water and offers micron level spatial resolution.

We have reported Raman spectra showing presence of both uncarbonated apatitic mineral and highly disordered carbonated mineral at the leading edge of fatigue-induced microcracks in bovine cortical bone [4] and at sites of catastrophic fractures in cortical bone subjected to bending [5]. These studies did not resolve whether the altered mineral phases were a cause or result of damage, that issue has now been successfully resolved. Recent indentation/Raman spectroscopic studies have confirmed our hypothesis of permanent local changes to both mineral and matrix resulting from

Correspondence to: M. D. Morris; E-mail: mdmorris@umich.edu

mechanical deformation [6]. These results are the first documented demonstration that the role of bone mineral in biomechanics extends beyond stiffening and suggests that alterations in mineral composition resulting from loading may toughen bone.

Hydrostatic pressure studies can further demonstrate cause/effect relations through collection of real time Raman data during mechanical loading, and can define pressure thresholds for spectral shifts as well as quantitative relations between pressure magnitude and spectral shifts. There have been no previous studies of high pressure Raman spectroscopy of bone. The technique, however, is widely used to study minerals, ceramics and polymers under conditions, such as those prevailing on the ocean floor or in the interior of the earth, and is also a convenient method for applying superphysiological loads [7]. Butler and coworkers have conducted extensive IR and Raman studies on pressure-induced changes in phosphate minerals, including hydroxyapatite, monocalcium phosphate and dicalcium phosphate [8–11], and there have been high pressure studies of calcium fluorapatite [12] as well as of calcite, aragonite and related carbonate minerals [13–15]. In this study, our aim was to examine the response (i.e., rate of change of the vibrational frequency of mineral and matrix bands as a function of applied pressure) of cortical bone subjected to hydrostatic compression and to compare the responses to those of a reference synthetic carbonated apatite. Using this experimental approach, we determined the relative response during loading and unloading of mineral vs. matrix, and within the mineral, phosphate vs. carbonate, as well as proteinated vs. deproteinated bone.

Materials and Methods

Specimens

Skeletally mature (6 mo. of age) murine (C57BL/6) and rat (Sprague-Dawley) femora (N = 3/condition) were harvested, stripped of soft tissue, wrapped in gauze and soaked in calcium-buffered saline at −32°C prior to handling. Both bone and deproteinated bone were analyzed. Condyles were sectioned off, and the mid-diaphyses of the bones were pulverized by snap freezing in liquid N_2 followed by grinding with mortar and pestle. Bone powders were stored in calcium-buffered saline at −32°C. Other bones were deproteinated in hydrazine with washing in ethanol. Deproteinated bone was stored at 4°C. Synthetic B-type carbonated apatite (~4% CO_3^{-2}) was prepared according to the procedure of Penel et al. [16]. Before each experiment, a small amount of the powder was dispersed and allowed to dry. The smallest visible crystallites (< 50 μm longest dimension) were recovered and used.

High Pressure Raman Spectroscopy

The bone mineral bands studied were the phosphate (PO_4^{-3}) ν_1 symmetric stretch (atmospheric pressure peak intensity 958 cm^{-1}) and the B-type carbonate (CO_3^{-2}) ν_1 symmetric stretch (1070 cm^{-1}). The bone matrix bands studied were markers for the collagen backbone, amide I (1655 cm^{-1}); methylene (CH_2) wag (1464 cm^{-1}) and methylene stretch (2937 cm^{-1}). Raman spectra were excited at 514.5 nm with an Ar^+ laser operating at 2 W focused to a 2 μm spot through an epi-illumination microscope with a 50× objective. The scattered radiation was analyzed with a spectrograph operated at 2 cm^{-1} resolution and a cooled CCD detector.

To study the hydrostatic compression of bone powder and related materials at pressures as high as 5 GPa we employed a Bassett-type diamond-anvil cell. The cell was fitted with rhenium gaskets 4 mm o.d. × 0.5 mm i.d. × 0.2 mm thick. The chamber was loaded with bone crystallites, and a drop of deionized water was added as coupling fluid. At each pressure increment the hydrostatic pressure inside the cell was monitored as the 2.9 cm^{-1}/GPa shift of the diamond Raman band at 1332 cm^{-1} [17]. *In situ* Raman spectra were collected in the 100-3800 cm^{-1} frequency range. Measurements were made under loading and unloading at pressure increments of approximately 200 MPa. Pressure changes were made by tightening or loosening screws on the chamber, and the elapsed time between changes was never less than 2 minutes.

Data Analysis

Spectra were baselined and bands were fitted to mixed Gaussian-Lorentzian line shapes to define band positions. Linear regression analyses of Raman shift wavenumber vs. applied pressure were applied to mineral and matrix bands for both loading and unloading regimes. Slopes dv/dP and intercepts $\nu_{P=0}$ were obtained from the linear fits.

Results

Raman spectra of powdered bone and a synthetic carbonated apatite reference mineral in the 900–1150 cm^{-1} region are shown for low (0–0.5 GPa) and high pressure (3.3–3.8 GPa) (Fig. 1). These spectra are representative of at least 3 samples. The spectral interval contains important Raman markers of bone mineral phosphate (957–958 cm^{-1}) and carbonate (~1070 cm^{-1}). The band shapes are typical of those observed at the low and high pressure regions of the pressure regime tested. For all specimens, shifts to higher wavenumbers are observed for both phosphate and carbonate bands as pressure is increased.

The phosphate envelopes for rat and mouse bones (Fig. 1b–1d) at low and high-pressures are similar, confirming that the observed effects are general and not unique to one species. There is always asymmetry in the band shape, with the low frequency side broader than the high frequency side. In some cases a shoulder at ca. 945 cm^{-1} is visible in addition to the band at 957–958 cm^{-1}. The bands become somewhat broader and the low frequency shoulder becomes more prominent with increasing pressure. This effect is most pronounced in the deproteinated bone where a low frequency shoulder is clearly visible at 3.6 GPa (Fig. 1b). The phosphate envelope for the synthetic carbonated apatite (Fig. 1a) is more symmetric and narrower than for the bone specimens. Comparison of the shapes and positions of band envelopes at atmospheric pressure for all specimens be-

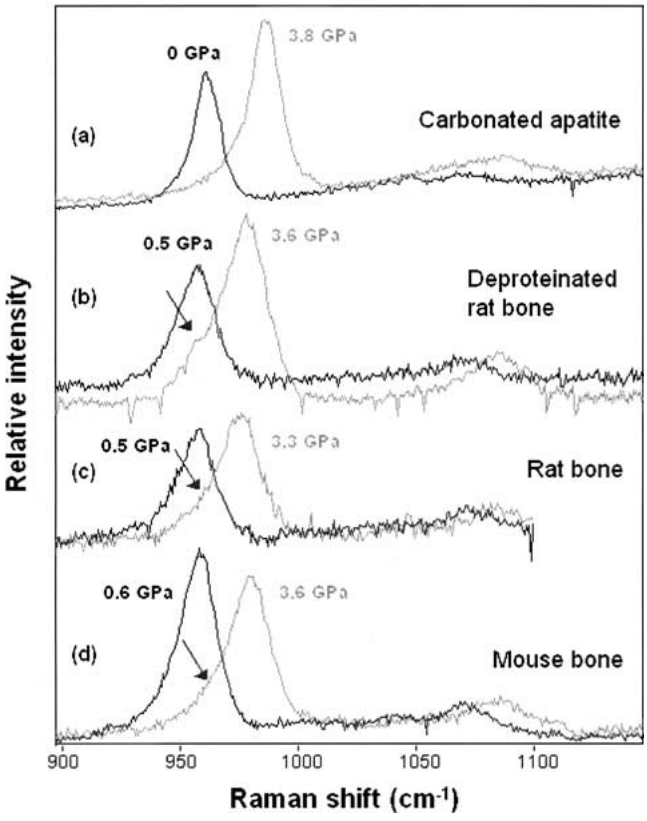

Fig. 1. Phosphate v_1 and B-type carbonate v_1 symmetric stretches for (**a**) synthetic B-type carbonated apatite (~4% CO_3^{-2}), (**b**) powdered and deproteinated rat bone, (**c**) powdered rat bone and (**d**) powdered mouse bone under low and high pressure.

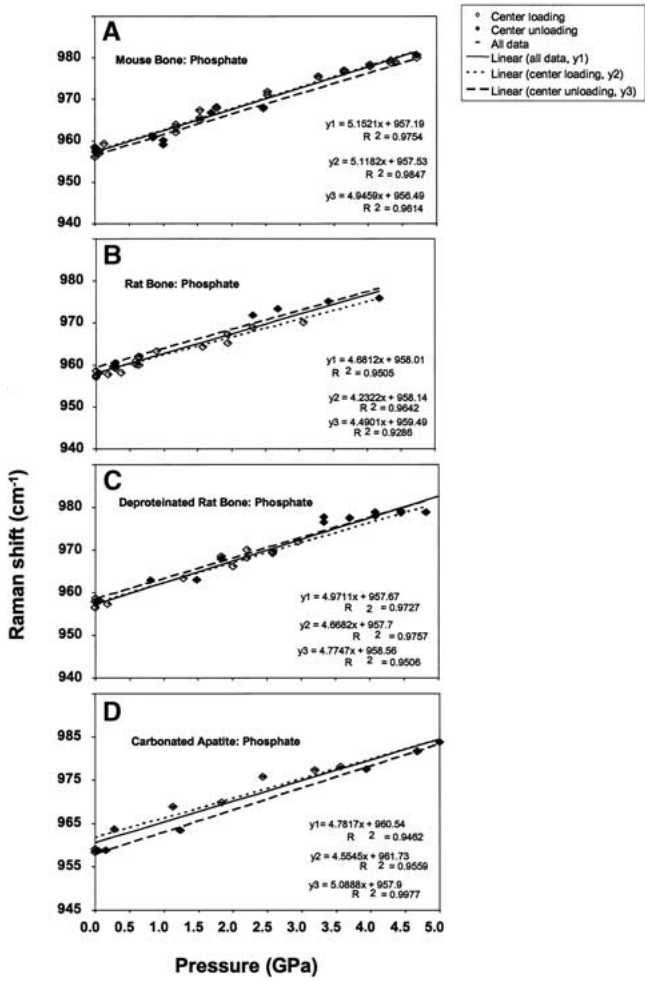

Fig. 2. Phosphate v_1 Raman shifts for (**A**) powdered mouse bone (**B**) powdered rat bone, (**C**) deproteinated rat bone, and (**D**) synthetic carbonated apatite versus pressure. All spectra were baseline-corrected. Loading: closed symbols and linear fit; unloading: open symbols and linear fit; all data: dashes and linear fit.

fore and after loading (not shown) revealed no permanent changes such as band shifts, band broadening or shoulders. Spectral changes are therefore reversible under the pressures applied in this investigation.

The phosphate v_1 pressure dependencies during loading and unloading are presented in Figure 2 for mouse bone, rat bone, deproteinated rat bone, and synthetic carbonated apatite. In Figure 3 the carbonate v_1 pressure dependences for the same specimens are shown. Linear regression analyses were applied to data in the loading and unloading regimes (Table 1). For the phosphate v_1 band of each type of specimen the slopes of the pressure dependence in loading and unloading are identical within $\pm 2\%$. The intercepts (atmospheric pressure Raman shift) are identical within ± 1 cm^{-1}, which is the experimental error. For mouse bone and deproteinated bone, the loading and unloading fits for carbonate v_1 show similar agreement. The collective data again demonstrate that the pressure-induced spectral changes are reversible.

Figure 4 shows the pressure dependencies for the matrix bands of mouse bone. Both the CH_2 wag and CH stretch shift to higher frequency with increasing pressure, although these bands have much larger pressure dependencies than do the mineral bands (Fig. 3). Amide I (collagen carbonyl stretching envelope) shifts to lower frequency, however. The slopes are smaller than those of other bands. Only for this band does the pressure dependence in unloading appear to differ from the dependence in loading.

Discussion

Many microstructural parameters, including crystal size, orientation and crystalline/amorphous ratio affect the mechanical properties of bone [2]. In order to understand the response of bone to mechanical loading, the microstructure must be defined. Microstructural analyses of murine cortical bone performed with wide angle x-ray scattering (WAXS) and TEM on sections of a similar location, age, gender and background strain as used in this study [18] are in agreement with what has been reported by others [2, 19]. Briefly, the microstructure of

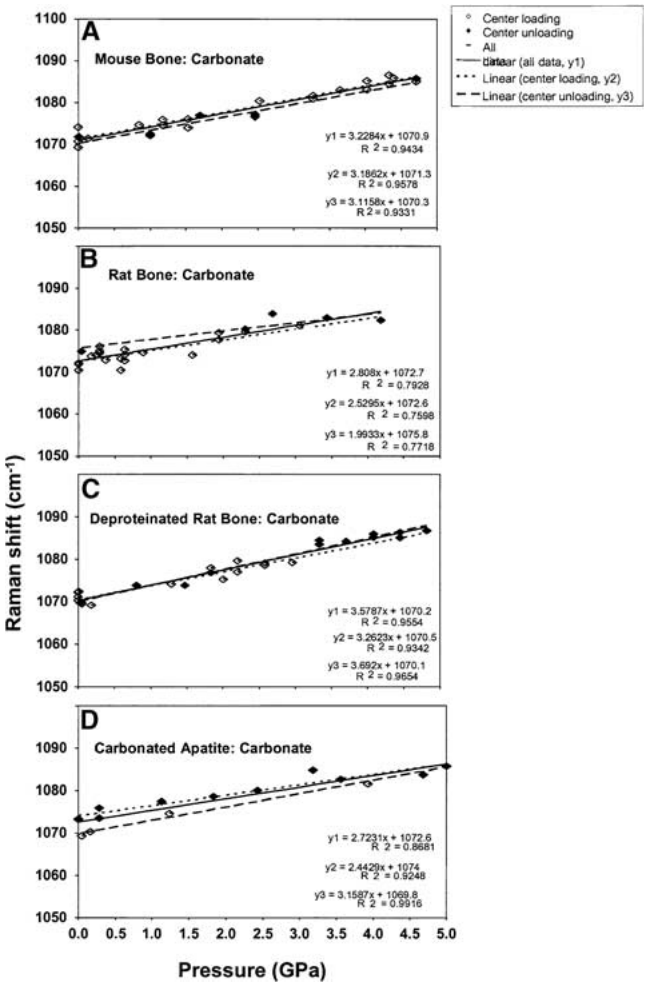

Fig. 3. Carbonate v_1 Raman shifts (**a**) Powdered mouse bone (**b**) powdered rat bone, (**c**) deproteinated rat bone, and (**d**) synthetic carbonated apatite versus pressure. All spectra were baseline-corrected. Loading: closed symbols and linear fit; unloading: open symbols and linear fit; all data: dashes and linear fit.

mid-diaphysial sections transverse to the long axis consists of needle-shaped crystals oriented primarily parallel to the axis. Crystals are approximately 2–3 nm thick and 50 nm long, and diffraction patterns are consistent with those of poorly crystalline carbonated apatite.

It is well-known that cortical bone is a highly-ordered material at every architectural level [2]. The order persists even in powdered tissue, such as used here, and would be expected to result in strongly polarization-dependent Raman spectra. However, because the tissue is powdered and a low numerical aperture objective that probes a relatively large volume is used, multiple scattering depolarizes the spectra, even if the crystallites are not completely randomly oriented. It is therefore probable that the sensitivity of the spectra to preferred crystallographic axes averages out, and isotropic assumptions are reasonable.

The change in vibrational frequency with pressure for carbonate is less than for phosphate. Since carbonate is known to be a rigid ion that cannot be greatly deformed, we propose, based on high pressure investigations of synthetic apatites and the theory presented below, that the pressure-induced shifts observed in the carbonate v_1 band are caused primarily by movement of anions and cations within the apatitic unit cell. As hydrostatic pressure increases, the crystallites become more compact.

The finding that phosphate $\partial v_i/\partial P$ exceeds carbonate $\partial v_i/\partial P$ is consistent with studies on synthetic minerals. For example, the phosphate $\partial v_i/\partial P$ in fluorapatite exceeds the carbonate $\partial v_i/\partial P$ in carbonates [13–15]. Moreover, the values of $\partial v_i/\partial P$ in this study are similar to those in the respective minerals reported elsewhere [13–15], suggesting that the structural changes governing the changes in vibrational frequency with pressure are similar. The structural changes in fluorapatite and carbonate as a function of pressure are well known. In particular, three structural features are important: the lattice compresses overall; the anions also compress; but the phosphate ion compresses more than the carbonate ion. This third feature is expected on crystal chemical grounds since the C-O bond in the carbonate group is much stronger than the P-O bond in the phosphate group.

The effect of pressure on the vibrational spectrum of a crystalline solid at constant temperature is commonly described by the isothermal mode Grüneisen parameter [18], given by equation 1,

$$\gamma_{iT} = \frac{K_T}{V_i}\left(\frac{\partial V_i}{\partial P}\right)_T \qquad (1)$$

where γ_{iT} is the isothermal mode Grüneisen parameter for the i^{th} vibrational mode of the material, v_i is the vibrational frequency of the i^{th} mode, K_T is the crystal bulk modulus, P is pressure and T is temperature. The theory predicts a linear dependence of vibrational frequency on pressure, but is only expected to be applicable for pressures that are small compared to the bulk modulus.

Depending on the mineral structure, pressure-dependent band shifts may arise from changes in the spacing of ions or other moieties in crystallites, from changes in hydrogen bonding, if there is any, or even from phase changes. Changes in oxy-anion X-O bond distances can occur but are unlikely to be major contributors for the small ions such as carbonate [20–22]. Most commonly, the spacing between ions is reduced. There is no requirement that γ_{iT} be constant for every vibrational band in a crystal. While adherence to equation 1 does not allow one to distinguish among several possible responses to pressure, it can be concluded that one mechanism is operative throughout the linear range.

The theory was developed for crystals consisting of monoatomic ions (e.g., NaCl, CaF_2) although it is

Table 1. Pressure dependence of bone Raman spectral bands

Specimen	Band assignment	$\nu_{P=0}$, cm^{-1}	$\nu_{P=0}$, cm^{-1} (loading)	$d\nu/dP$ (loading)	R^2	$\nu_{P=0}$, cm^{-1} (unloading)	$d\nu/dP$ (unloading)	R^2
Mouse bone	PO_4^{-3} ν_1	958 ± 1	957.5	5.118	0.985	956.5	4.946	0.961
Rat bone	PO_4^{-3} ν_1	958 ± 1	958.1	4.232	0.964	959.5	4.490	0.929
Deproteinated rat bone	PO_4^{-3} ν_1	958 ± 1	957.7	4.668	0.976	958.6	4.775	0.951
Carbonated apatite	PO_4^{-3} ν_1	959 ± 1	961.7	4.554	0.956	957.9	5.089	0.998
Mouse bone	CO_3^{-2} ν_1	1072 ± 2	1071.3	3.186	0.958	1070.3	3.116	0.933
Rat bone	CO_3^{-2} ν_1	1073 ± 2	1072.6	2.530	0.760	1075.8	1.993	0.772
Deproteinated rat bone	CO_3^{-2} ν_1	1071 ± 1	1070.5	3.262	0.934	1070.1	3.692	0.965
Carbonated apatite	CO_3^{-2} ν_1	1072 ± 2	1074	2.443	0.925	1069.8	3.159	0.992
Mouse bone	CH_2 wag	1455	1457.9	6.612	0.967	1459.2	5.548	0.921
Mouse bone	amide I	1654 ± 3	1654.1	−1.730	0.510	1649.5	-0.676	0.458
Mouse bone	CH_2 stretch	2937 ± 4	2934	8.269	0.944	2934.3	7.365	0.997

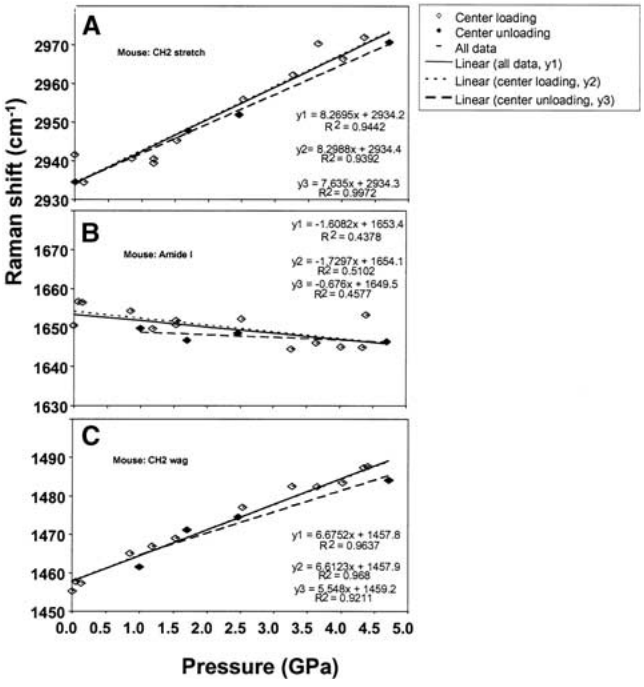

Fig. 4. Raman shifts in powdered mouse bone for (**a**) Amide I, (**b**) methylene stretch and (**c**) methylene wag versus pressure. All spectra were baseline-corrected. Loading: closed symbols and linear fit; unloading: open symbols and linear fit; all data: dashes and linear fit.

commonly applied to crystals containing polyatomic ions such as phosphates, carbonates and silicates, with a clear understanding that simple theories cannot be rigorously correct [20] even though the equations are useful descriptions of experimental observations. The mode Grüneisen parameter equation can be extended to include crystals containing polyatomic ions [23],

$$\gamma_{iT} = \frac{K_X}{V_i}\left(\frac{\partial V_i}{\partial P}\right)_T \qquad (2)$$

where K_X is the polyhedral bulk modulus associated with the vibrating moiety, such as a phosphate or carbonate ion. The extended mode Grüneisen parameter equation also predicts a linear dependence of vibrational frequency on pressure, but accounts for differences in pressure response caused by, for example, compression of oxyions. Because of the utility of the Grüneisen parameter concept, it is used as a convenient semi-empirical approach to help interpret experimental data and postulate the structural changes that occur as the bone crystallites are subjected to pressure, not as an exact theory for bone deformation.

This simple theory of inorganic crystal pressure dependence predicts that pressure dependence will be linear. To the extent that all vibrations contribute equally to the expansion of the crystal, the isothermal mode Grüneisen parameter as defined in formula (1) should be the same for all modes and the slope of the vibrational frequency vs. pressure should vary inversely with the frequency of the mode. Because phosphate $\nu_1 \sim 958\ cm^{-1}$, and carbonate $\nu_1 \sim 1071\ cm^{-1}$, $\partial\nu/\partial P$ for the two bands should differ by about 12%. Instead, $d\nu_1/dP$ of carbonate is at least 59% less than that of phosphate. This difference can be understood on the basis of the extended mode Grüneisen equation (2): the polyhedral bulk modulus of the carbonate ion is greater than that of the phosphate ion [24]. As the stiffer ion deforms less with increasing pressure, its vibrational frequency changes comparatively little. In addition to deformation of the ions, other deformation mechanisms may influence vibrational frequencies, particularly for the less rigid phosphate ion. For example, Xu et al. [8] have suggested that in hydroxyapatite the hydroxide ions move under pressures above 3 GPa. There is less hydroxide in bone than in hydroxyapatite [25]. Nonetheless, movement of any hydroxide would influence the larger phosphate, some of which is adjacent to the column of remaining hydroxide, more than the smaller carbonate. Comodi et al. [14, 15] have correlated the results of high pressure X-ray diffraction and high pressure Raman spectroscopy. They find that compression is mostly a change of anion/cation spacing, but

compression of the phosphate ion itself is about 1/3 as great as compression of the lattice.

No permanent changes such as band broadening or shoulders were observed when the specimens were returned to atmospheric pressure, and the slopes of the loading and unloading regimes for phosphate were equivalent. The phosphate peak frequency returned to within ± 1 cm^{-1} of its initial value. Together these observations show that under the conditions imposed in this study, the changes are reversible or that the fraction of conversion is too small to measure [26].

Carbonate v_1 has lower intensity than phosphate v_1. While in many of our specimens there is good agreement between the loading and unloading slopes, the 23% discrepancy between loading and unloading in rat bone may be more a result of experimental error in measurement of a weak and broad band rather than evidence for irreversibility. However, the data are noisy and the correlation coefficients are low (0.76–0.77), so we cannot definitively conclude that the pressure effect for carbonate is irreversible.

The phosphate band envelope for the synthetic carbonated apatite is more symmetric and narrower than for the bone specimens, as expected for a more ordered crystal such as carbonated apatite. This mineral is more homogeneous and more crystalline (mineral crystallinity $\cong$0.083 cm) than the highly impure and variable natural mineral (bone mineral crystallinity $\cong$0.06 cm).

There is a difference in response of bone to hydrostatic pressure vs. axial loading or bending. We have previously reported irreversible changes to bone mineral under conditions that cause permanent damage, ranging from microcrack formation to fracture [4–6]. Permanent change may involve insertion into or loss of water from the crystal lattice. Bone mineral crystallites are known to be only one or two unit cells thick [27–29]. Because of the small size, movement of water or ions into or out of the lattice is not as difficult as it would be in large crystallites. Under hydrostatic conditions, however, it would be difficult to move either water or ions into or out of crystallites because pressure is applied uniformly in all directions. As a result, changes in vibrational frequency are reversible.

Details of the response of collagen to pressure remain unclear. One would not expect a simple pressure dependence for any band in the spectrum of a protein that includes some three thousand amino acids. Indeed, most of the bands in the spectrum are really superpositions of many of the closely spaced bands. Some of the band envelopes are resolvable into several components, most notably the amide I and amide III envelopes, for which several maxima or shoulders have been identified with particular secondary structure domains [30] or state of interfibril cross-links [31]. Because of the complexity of this problem, our discussion is empirical and our conclusions are only preliminary.

The large changes in methylene wag frequency are consistent with either changes in the pitch of the collagen helix or with changes in interfibril links. The Amide I data suggest irreversible changes to protein secondary structure, but are insufficient to prove them. If irreversible changes to collagen are found, this behavior would contrast with behavior observed during indentation [6], where collagen fibrils were found to be resistant to compression-induced damage.

Because of the width of the Amide I envelope, the low signal to noise ratio and the poor fit (R^2 0.46–0.51), we cannot conclude that the pressure dependence is reversible or irreversible, or even that it is linear. However, when the system is returned to atmospheric pressure after imposition of high pressure, this band, a sensitive marker for changes in matrix cross-links, returns to its original shape, suggesting that the process is reversible.

The weak pressure dependence observed for Amide I is surprising because this band responds to changes in secondary structure and hydrogen bonding. However, as discussed above, Amide I is actually a composite of several bands, representing an average response of many C-O bands and cross-links. The Amide I response contrasts with the very large positive pressure dependences of the CH_2 wag and the CH_2 stretch bands. We propose that the Amide I (and possibly CH_2 wag) is shielded from the effect of bulk water and that the internal H-bonding is stronger and more stable. Amide I is in contact with a very thin layer of internal water which would not respond identically to pressure as bulk water, hence, the different response to compression from the other bone components.

In all experiments, we were able to obtain more data points in loading than in unloading. We were able to collect data at 20–30 pressure magnitudes during loading, but only 8–10 pressures during unloading. Pressure reduction causes release of gas bubbles in the diamond anvil cell. In many cases bubble formation caused sufficient reduction in the intensity of collected Raman scattered light to render band positions unmeasurable.

In summary, diamond anvil cell studies on bone complement the Raman changes associated with microcracks, indentation and dynamic mechanical tests [4–6], as we have previously reported, and suggest that bone responds actively to mechanical stress in more complex ways than have previously been recognized. The change in vibrational frequency with pressure for the more rigid carbonate is less than for phosphate, and caused primarily by movement of ions within the unit cell. Deformation of phosphate on the other hand, results from both ionic movement as well as distortion. Changes in vibrational frequencies of organic species with pressure are greater than for mineral species, and are consistent with changes in protein secondary structure such as alterations in interfibril cross-links and helix

pitch. Changes in vibrational frequency with pressure are similar between loading and unloading, implying reversibility, as a result of the inability to permanently move water out of the lattice.

Acknowledgments. This research was supported in part through NIH grants P30 AR46024 (MDM), R01 AR047969 (MDM), T32 DE07057 (DHK) and DoD/Dept. of the Army, DAMD 17-03-1-0556 (DHK).

References

1. Kaplan FS, Hayes WC, Keaveny TM, Boskey A, Einhorn TA, Iannotti JP (1994) Form and function of bone. Orthopaedic Basic Science. American Academy of Orthopaedic Surgeons, Rosemont, pp 127–184
2. Weiner S, Traub W, Wagner HD (1999) Lamellar bone: structure-function relations. J Struct Biol 126:241–255
3. Carden A, Morris MD (2000) Application of vibrational spectroscopy to the study of mineralized tissues. J Biomed Optics 5:259–268
4. Timlin JA, Carden A, Morris MD, Rajachar RM, Kohn DH (2000) Raman spectroscopic imaging markers for fatigue-related microdamage in bovine bone. Anal Chem 72:2229–2236
5. Morris MD, Carden A, Rajachar RM, Kohn DH (2002) "Effects of applied load on bone tissue as observed by Raman spectroscopy". In: Mahadevan-Jansen A, Mantsch HH, Puppels GJ (eds), *Biomedical vibrational spectroscopy II*, Spie Press, Vol. 4614, Bellingham, WA, pp 47–54
6. Carden A, Rajachar RM, Morris MD, Kohn DH (2003) Ultrastructural changes accompanying the mechanical deformation of bone tissue: a Raman imaging study. Calcif Tissue Int 72:166–175
7. Ferraro JR (1984) Vibrational spectroscopy at high external pressures. Academic Press, Xiv, pp 264
8. Xu JW, Gilson DFR, Butler IS, Stangel I (1996) Effect of high external pressures on the vibrational spectra of biomedical materials: calcium hydroxyapatite, calcium fluoroapatite. J Biomed Mater Res 30:239–244
9. Butler IS, Gilson DFR (1997) Recent studies of the high-pressure vibrational microspectra of solid inorganic materials. J Molec Struct 408:39–45
10. Xu JW, Gilson DFR, Butler IS (1998) FT-Raman and high-pressure FT-infrared spectroscopic investigation of monocalcium phosphate monohydrate, $Ca(H_2PO_4)_2{\cdot}H_2O$. Spectrochim Acta A Mol Spectrosc 54:1869–1878
11. Xu JW, Butler IS, Gilson DFR (1999) FT-Raman and high-pressure infrared spectroscopic studies of dicalcium phosphate dihydrate ($CaHPO_4$ $2H_2O$) and anhydrous dicalcium phosphate ($CaHPO_4$). Spectrochim Acta 55A:2801–2809
12. Williams Q, Knittle E (1996) Infrared and Raman spectra of $Ca_5(PO_4)F_2$ - fluorapatite at high pressures: compression-induced changes in phosphate site and Davydov splittings. J Phys Chem Solids 57:417–422
13. Gillet P, Biellmann C, Reynard B, McMillan P (1993) Raman-spectroscopic studies of carbonates. 1. High pressure and high temperature behavior of calcite, magnesite, dolomite and aragonite. Phys Chem Miner 20:1–18
14. Comodi P, Liu Y, Zanazzi PF, Montagnoli M (2001) Structural and vibrational behavior of fluorapatite with pressure. Part I. In situ single-crystal x-ray diffraction investigation. Phys Chem Minerals 28:219–224
15. Comodi P, Lin Y, Frezzotti ML (2001) Structural and vibrational behaviour of fluorapatite with pressure. Part II. In situ micro-Raman spectroscopic investigation. Phys Chem Miner 28:225–231
16. Penel G, Leroy G, Key C, Bres E (1998) Micro-Raman spectral study of the PO_4 and CO_3 vibrational modes in synthetic and biological apatites. Calcif Tissue Int 63:475–481
17. Boppart H, van Straaten J, Silvera IF (1985) Raman spectra of diamond at high pressure. Phys Rev B 32:1423–1425
18. Rajacher RM, Garden A, Morris MD, Kohn DH (2001) Ultrastructural-level characterization of microdamage in cortical bone using Raman spectroscopy and WAXS, In: Advances in bioengineering, BED-Vol 50, pp 309–310
19. Fratzl P, Groschner M, Vogl G, et al. (1992) Mineral crystals in calcified tissues: a comparative study by SAXS. J Bone Min Res 7:329–334
20. Gillet P, Hemley RJ, McMillan PF (1998) "Vibrational properties at high pressures and temperatures." In: HYemley RJ (ed), *Ultra-High Pressure Minerology*, Mineralogical Society of America, Washington, DC, pp 525–590
21. Ross Nl (2002) "Framework structures". In: Hazen, Rm, Downs, RT (editors), *High-Temperature, High-Pressure Crystal Chemistry*, Mineralogical Society of America, Washington, DC, pp 257-287
22. Stixrude L, Cohen RE, Hemley RJ (1998) "Theory of minerals at high pressure". In: Hemley RJ (ed), *Ultra-High Pressure Mineralogy*, Mineralogical Society of America, Washington, DC, pp 639–671
23. Hofmeister AM, Mao H-K (2002) Redefinition of the mode Grüneisen parameter for polyatomic substances and thermodynamic implications. Proc Nat Acad Sci 99:559–564
24. Hazen RM, Finger LW (1982) Comparative Crystal Chemistry. John Wiley and Sons, New York
25. Cho G, Wu Y, Ackerman JL (2003) Detection of hydroxyl ions in bone mineral by solid-state NMR spectroscopy. Science 300:1123–1127
26. Xu J-A, Mao Moissanite H-K (2000) A window for high-pressure experiments. Science 290:783–785
27. Eppell SJ, Tong W, Katz JL, Kuhn L, Glimcher MJ (2001) Shape and size of isolated bone mineralites measured using atomic force microscopy. J Orthopaed Res 19:1027–1034
28. Tong W, Glimcher MJ, Katz JL, Kuhn L, Eppell SJ (2003) Size and shape of mineralites in young bovine bone measured by atomic force microscopy. Calcif Tissue Int 72:592–598
29. Rubin MA, Jasiuk I, Taylor J, Rubin J, Ganey T, Apkarian RP (2003) TEM analysis of the nanostructure of normal and osteoporotic human trabecular bone. Bone 33:270–282
30. Lazarev YA, Grishkovsky BA, Khromova TB (1985) Amide I band of IR spectrum and structure of collagen and related polypeptides. Biopolymers 24:1449–1478
31. Paschalis EP, Verdelis K, Doty SB, Boskey AL, Mendelsohn R, Mamauchi M (2001) Spectroscopic characterization of collagen cross-links in bone. J Bone Miner Res 16:1821–1828